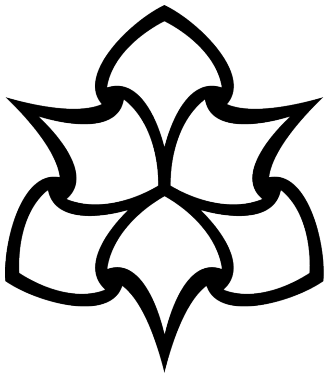

IEEE Access
Multidisciplinary | Rapid Review | Open Access Journal

Received April 27, 2021, accepted May 17, 2021, date of publication May 26, 2021, date of current version June 10, 2021.

*Digital Object Identifier 10.1109/ACCESS.2021.3083937*

# Acoustical Characteristics of Proton Exchange Membrane Fuel Cells

**MOHMAD AL-RWEG[1], KHALED AHMEDA[2], AND ALHUSSEIN ALBARBAR[1], (Member, IEEE)**

[1]Smart Infrastructure and Industry Research Group, Department of Engineering, Manchester Metropolitan University, Manchester M15 6BH, U.K.
[2]Cardiff School of Technologies, Cardiff Metropolitan University, Cardiff CF5 2YB, U.K.

Corresponding author: Mohmad Al-Rweg (m.alrweg@mmu.ac.uk)

**ABSTRACT** In order to optimise the performance of Proton Exchange Membrane Fuel Cells (PEMFCs) and to maximise their life cycle, water content has to be properly controlled. This paper presents a model-based method to determine the effect of load on PEMFC water content in PEMFCs using Acoustic Emission (AE) measurements. The developed model was implemented in COMSOL and verified using a single proton exchange membrane fuel cell (FC) operated under various loads. Acoustical events originating from water bubble formation have been identified and assessed using statistical parameters determined in the time and frequency domains. The feasibility of using AE techniques to detect and monitor the impact of a cell's load variation on water content is assessed. As the model results were in good agreement with experimental data, it was concluded that an AE based method could serve as an effective monitoring and control tool of water content in PEMFCs. Statically, the root mean square for acoustic emission activity has a significant relation with load characteristics and can, potentially, be a candidate for determining the AE behavior in a PEMFC.

**INDEX TERMS** PEM fuel cells, acoustic emissions, condition monitoring.

## I. INTRODUCTION

It has been observed that the world's total energy consumption was 22,536 TWh in 2020 and sustainable energy's share was projected at 13.5 % [1]. However, approximately 86.5 % of all the usable global primary energy was fossil fuel-based, especially coal, oil, and natural gas [2]. The use of conventional fuels as sources of energy is not encouraged due to their greenhouse gas emissions, and one solution proposed is to replace fossil fuels with clean, sustainable, and eco-friendly energy sources.

Therefore, the global demand for alternative energy resources is growing daily due to numerous issues. The most important of which are: depletion of fossil fuels,global warming, and pollution. Increasing oil prices and the negative environmental effects of fossil fuels are undeniable. The effect of this is compounded by the global concerns of adverse environmental effects of fossil fuel consumption dependency. These are the primary driving forces behind the global pursuit for clean and sustainable energy obtained from renewable resources such as solar, wind energy, and green hydrogen technologies [3]. This is becoming even more important as by 2040, it is projected global energy consumption will rise by 36 %.

The hydrogen economy may assist with the above-mentioned issues as hydrogen is a renewable resource that can be produced from electrolysis of water using the electricity derived from green sources such as photovoltaics, wind, and bioenergy sources. Hydrogen is seen as an attractive alternative since pure water is a by-product when it reacts with oxygen in a fuel cell. Thus, hydrogen and fuel cell technologies can address two of the essential challenges, reducing carbon dioxide emissions and overall dependence on fossil fuels [4].

As a core technology of a hydrogen economy, fuel cells (Figure 1) will play a vital role in offering a cleaner, more efficient alternative to gas and steam turbines at distributed power generation stations. However, to date, the cost, efficiency, and reliability of fuel cells (FCs) are not comparable to gas or steam turbines [5]–[7].

Over the last 50 years, a significant amount of research has been conducted in order to develop highly efficiency and environmentally friendly fuel cells. However, performance has been only slightly enhanced, and durability and reliability have not demonstrated major improvements. This has meant

The associate editor coordinating the review of this manuscript and approving it for publication was Zhouyang Ren.

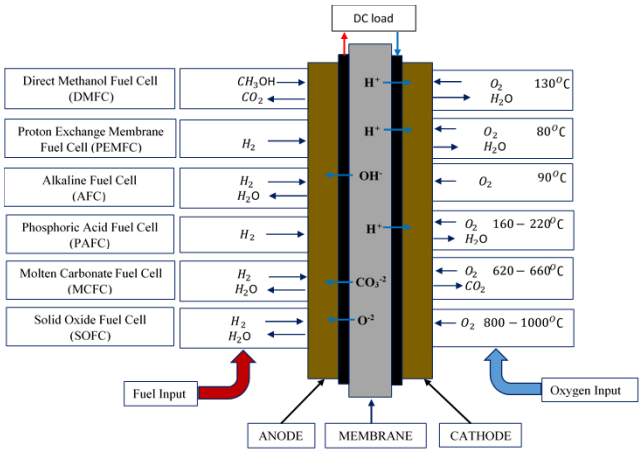


**FIGURE 1.** The functionalities of fuel cells.

fuel cells have not been widely adopted because of their relatively low durability and reliability, and unacceptably high cost [8]–[10]. One obstacle in the way of improving the performance and reliability of fuel cells is an inadequate understanding of the phenomena that occur within them, due mainly to their complexities. The study and investigation of these complexities will greatly assist in determining solutions amongst many problems related to fuel cells including water management.

The acoustic characteristics of fuel cells, if fully understood, may lead to significant improvements in their design, control, durability, and reliability. Chemical reactions that occur in fuel cells are accompanied by energy transfer, with some of that energy converted into acoustic signals. One possible acoustic source is the activity of bubbles which occur due to the electrochemical reactions between fuel ($H_2$) and oxidiser ($O_2$) forming water at the cathode side. The rate of formation of the bubbles is closely related to the speed of the chemical reaction. A fast-electrochemical reaction will lead to high rate of bubble formation, and consequently, an increase in the amplitude of acoustic emission (AE). Thus, the AE signals may carry very useful information about the condition of PEMFCs and the factors influencing their operation.

In the literature, AE techniques are widely used in electromechanical systems. For example, AEs have been utilized to monitor and examine combustion [11], [12]; electrochemical phenomena such as anodization, corrosion and even oxygen reduction [13]. However, only a few studies have investigated this phenomenon in fuel cells. Crowther *et al.* investigated acoustic signals induced in electrolyzers and found substantial emissions at approximately 800 kHz due to the decomposition of water molecules [14]. However, that study focused only on the electrochemical reactions that occurred within the electrolyzer and the resulting power spectrum of the AE signals.

In more recent work, Legros *et al.* [15] used electrochemical impedance spectroscopy and AE measurements to assess the health of PEMFCs. By deriving an electrical equivalent circuit, they managed to detect and assess the effects of flooding.

Maier *et al.* [16] utilised the AE technique to study the gaseous flow inside PEMFCs. The study concluded that there are good correlations between the flow rates, current quantity and the corresponding AE parameters measured.

Recently Saad Saleem Khan *et al.* [17] proposed a developed model based on the quantum lightning search algorithm (QLSA). In this study, PEMFC was opening under various operating condition such as temperature and humidity. This work concluded that cell voltage varies with the ambient and load variation. In addition, the model can predict the water content of the membrane.

Dong-Hoon Shin et al, [18] used a real-time monitoring technique to assess the water content in PEMFC. Randle's equivalent electrical circuit was used to measure the voltages of the cell from which can be used to distinguish between flooding and drying condition based on the value of membrane resistance and activation resistance corresponding to the equivalent circuit model.

Based on the above literature survey, no rigorous research has investigated and characterized the acoustical behavior of PEMFCs, and a clear understanding of such behavior is timely needed. This paper attempts to provide a deeper analysis of acoustic emission signals generated by PEMFCs and data analysis via realistic modelling and experimental validation.

Water formation and importance of management in PEMFC are explained in Section 2. Section 3 explains the acoustic emissions signals generation mechanisms in PEMFC. A realistic mathematical model is derived to understand intensity and frequency bands of the emitted acoustic signals under normal and abnormal conditions. The experimental setup and instrumentation are explained in Section 4, which also describes the collection of empirical data for model validation purposes. Results and discussions are provided in Section 5, model-based, predicted acoustical behavior was compared to experimentally measured data for verification and to direct further research. Conclusions and suggestions for future work are provided in Section 6.

## II. WATER FORMATION AND MANAGEMENT

The accumulation of water in a fuel cell is the result of electro-osmotic drag and back diffusion. Electro-osmotic drag happens when protons carry water droplets from anode to the cathode across the membrane which can subsequently lead to a cell flooding. Back diffusion occurs as due to a water concentration gradient existing across the cathode and anode, leading to water drops moving from cathode to the anode. This consequentially, results in the drying of the membrane. Membrane thickness and its water content can be used to estimate the water concentration gradient between both sides of the cell as well as the humidity of the reactant gases. Both electro-osmotic drag and back diffusion are key factors in determining current density. At a high current density, the impact of electro-osmotic drag will be higher than the

effect of back diffusion, while at a low current density back diffusion is comparable to the electro-osmotic drag. Thus, usually, the anode tends to be dry even if the cathode is well hydrated at low current density.

Water management is needed to resolve the inherent contradiction of ensuring high membrane conductivity while protecting the cell from flooding [6].

During the normal operation of PEMFCs, water is produced at the cathode side as a result of electrochemical reactions. A proportion of this water is used to humidify the membrane and enhance its ionic conductivity, and the remainder is removed. The main function of the membrane is to prevent the electrons passing from one side to the other, permitting only positive and negative ions and water molecules to pass through. If water production rates exceed removal rates, water will flood and block the membrane pores and gas diffusion layers (GDLs). This leads to cell degradation due to gas starvation at both electrodes. Mass transport losses are closely related to flooding, especially at the cathode side, because the transport rates of the reactants to the electro-catalyst layers are significantly reduced [20]. The output voltage can be recovered quite fast, as soon as both sides of the cathode and anode are purged. Therefore, adequate humidification for good conductivity and low resistance losses must be maintained while flooding is avoided. It is normal practice to assume that in the GDLs, the catalyst layers (CL), and membranes are at the same temperatures and that membrane conductivity ($\lambda$) and water content ($a_{water_{vap}}$) can be described by Equation 1 [21]:

$$\lambda = 0.043 + 17.18a_{water_{vap}} - 39.85(a_{water_{vap}})^2 + 36(a_{water_{vap}})^3 \quad (1)$$

The value of $a_{water_{vap}}$ can be computed using Equation 2:

$$a_{water_{vap}} = \frac{P_w}{P_{sat}} \quad (2)$$

where $P_w$ denotes the partial pressure of water vapor and $P_{sat}$ is the saturation water vapor pressure and can be determined using Equation 3 [20], where T is temperature of the cell, measured in K:

$$P_{sat} = 0.161121(exp(17.123\frac{1}{T + 234.95})) \quad (3)$$

Water accumulation of the cathode with respect to the anode ($\alpha$) can be approximated by the linear difference of a single step as shown in Equation 4 [21]:

$$\alpha = n_{drag} - \frac{F}{I_a}D_w - \frac{C_{w,c} - C_{w,a}}{t_m} \quad (4)$$

where $t_m$ is the thickness of the membrane, $n_{drag}$ is the electro-osmotic drag coefficient, which is the same as the number of water molecules carried by a proton.

The quantity $\alpha$ is highly dependent on the water content of the given membrane, which is a function of the water activity in the gas phase adjacent to the membrane. The partial dehydration that exists along the anode, as well as the saturation that exists along the cathode, are more likely to occur at higher current densities. This is due to the higher transport rate of water due to the electro-osmosis drag from the anode to cathode, compared to the back-diffusion rate of water from the cathode to the anode. Physically, this means that the water content on the anode side is lower. However, the water activity on the anode side may be used to calculate the electro-osmotic coefficient in the membrane. The electro-osmotic coefficient is a function of the water activity in the lower channel of the anode used and can be expressed by Equation 5. The water content will also be limited by water activity as described in Equation 5 [21]:

$$\lambda = \begin{cases} 0.043 + 17.18a - 39.85a^2 + 36a^3 & for\ 0 < a \leq 1 \\ 14 + 1.4\,(1 - a) & for\ 1 < a \leq 3 \end{cases} \quad (5)$$

Equation (5) can be rewritten as Equation 6:

$$\lambda = \begin{cases} 14a & for\ 0 < a \leq 1 \\ 12.6 + 1.4a & for\ 0 < a \leq 3 \end{cases} \quad (6)$$

The flooding of the cathode is associated with three mechanisms:

a) The influence of applied electricity that occurs at the membrane causing electro-osmotic drag results in the movement of protons from the negative to positive, carrying water molecules with them, particularly at high current loads. The current density in the cathode increases as the relative humidity at the membrane increases because of electron conductivity.
b) Water forms due to the reaction between fuel molecules and oxidizer molecules at the cathode. The water level increases when the load and/or current density increases.
c) Liquid water injection and saturated reactant gases contribute to flooding.

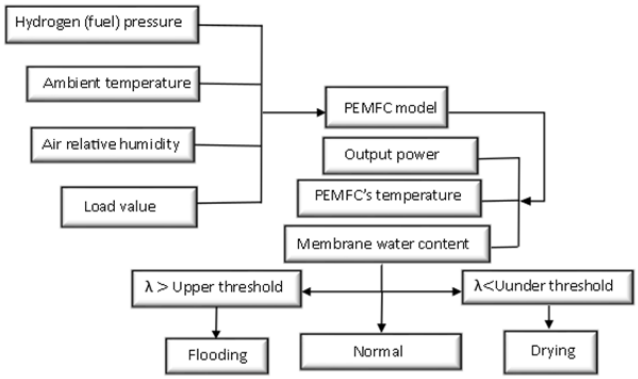


**FIGURE 2.** PEMFC water management philosophy flow chart.

## III. ACOUSTIC EMISSION GENERATION IN PEMFCS

The main source of AE signals is the oscillation of water bubbles and friction between them. Minnaert's resonance equation can be used to find the resonant frequencies $f_o$ of

a bubble with a particular radius as shown in Equation 7 [21]:

$$f_o = \frac{1}{2\Pi a}\left(\frac{3\Upsilon p_a}{\rho}\right)^{1/2} \tag{7}$$

where :$a$ is the radius of the bubble, $p_a$ is the ambient pressure, $\rho$ is the density of the water and $\Upsilon$ is the polytrophic coefficient.

Re-arranging Equation 7 gives Equation 8, which presents the volume of a bubble in terms of its resonant frequency:

$$V = \frac{1}{(6*\pi^2*f_o)} * \left(\frac{3 * \gamma * p_a}{\rho}\right)^{3/2} \tag{8}$$

**TABLE 1. Bubble radius and volume as derived from resonant frequency.**

| Frequency (kHz) | Bubble radius (mm) | Bubble volumes ($mm^3$) |
|---|---|---|
| 100 | 0.086953 | 2.7539e-03 |
| 200 | 0.043477 | 3.4424e-04 |
| 300 | 0.028984 | 1.0200e-04 |
| 400 | 0.021738 | 4.3030e-05 |
| 500 | 0.017391 | 2.2031e-05 |
| 600 | 0.014492 | 1.2750e-05 |
| 650 | 0.013377 | 1.0028e-05 |
| 700 | 0.012422 | 8.0289e-06 |
| 750 | 0.011594 | 6.5278e-06 |
| 800 | 0.010869 | 5.3787e-06 |
| 850 | 0.010230 | 4.4843e-06 |

Table 1 shows the induced frequencies $f_o$ of a water bubble with a particular radius and volume, in each electrochemical reaction stage. Figure 3 illustrates the relationship between induced frequency and bubble size.

It is possible to experimentally measure a particular peak frequency than table 1 and Figure 3 can be used to estimate the size of the bubble generating that frequency.

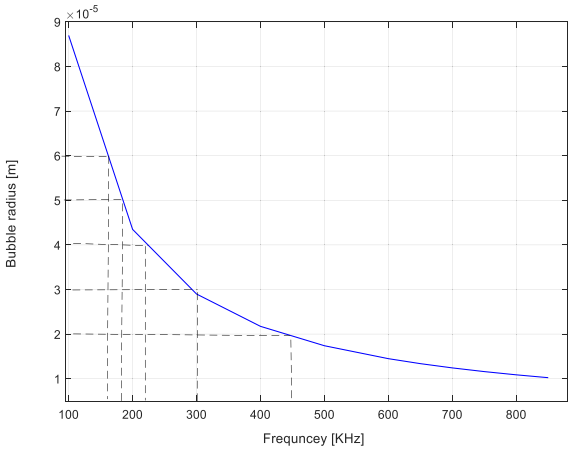


**FIGURE 3. Relationship between frequency and bubble size.**

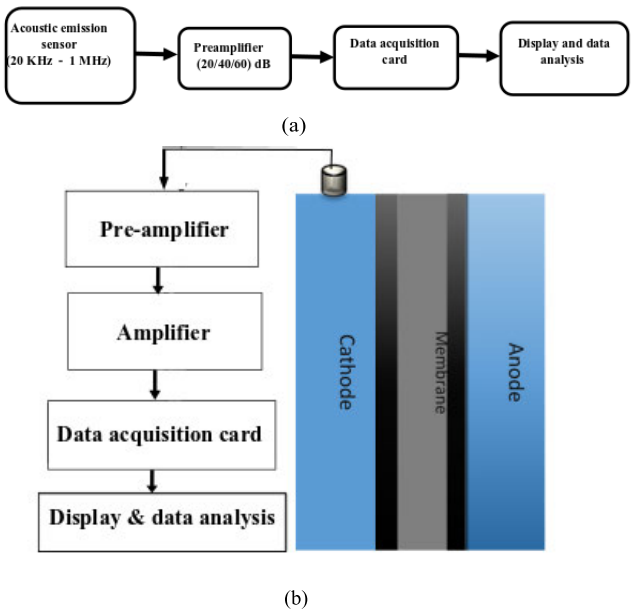


**FIGURE 4. a. Block diagram of the AE signal measuring system. b. The experimental setup.**

## IV. EXPERIMENTAL SETUP AND DATA COLLECTION

The test rig used in this work comprised a single PEMFC with 500 mW maximum output power and Nafion 115 serving as the membrane with a thickness 127 $\mu$m and active area of 9 $cm^2$. The catalyst layer was 50 $\mu$m thick, giving a total electrode thickness of 0.25 $\pm$ 0.02 mm. The catalyst layer was made of carbon-supported platinum with a loading of 1 $mg/cm^2$. The membrane electrode assembly was first sandwiched between gasket and then between two graphite current collector plates. Flow channels were included on each plate surface. Finally, all of the elements were sandwiched between two metal current collector plates. Humidified hydrogen and air were used as fuel and oxidant, respectively. AE parameters are strongly affected by the density of the current. Five different loads were applied: 20%, 40%, 60%, 80%, and 100% of the cell's full load, in order to investigate the levels of AE signals.

In order to approach the source of acoustic emission events and ensure an effective acoustic coupling, AE sensor was mounted on top of the PEMFC (cathode side), see Figure 4a. The sensor was attached using special wax, which supported the sensor during the experiment and supplied the necessary acoustic coupling.

The data system utilized to collect information from the PEMFC system comprised the piezoelectric sensor and preamplifier. Due to the large frequency range of the AE spectrum (typically ranging from 20 kHz to 1 MHz), an Acoustic Technology Group sensor, model NS2000m, was used to gather data from the PEMFC system. The output of the sensor was connected to a preamplifier with 20 kHz – 5 MHz bandwidth, which amplified the signal from the sensor and was

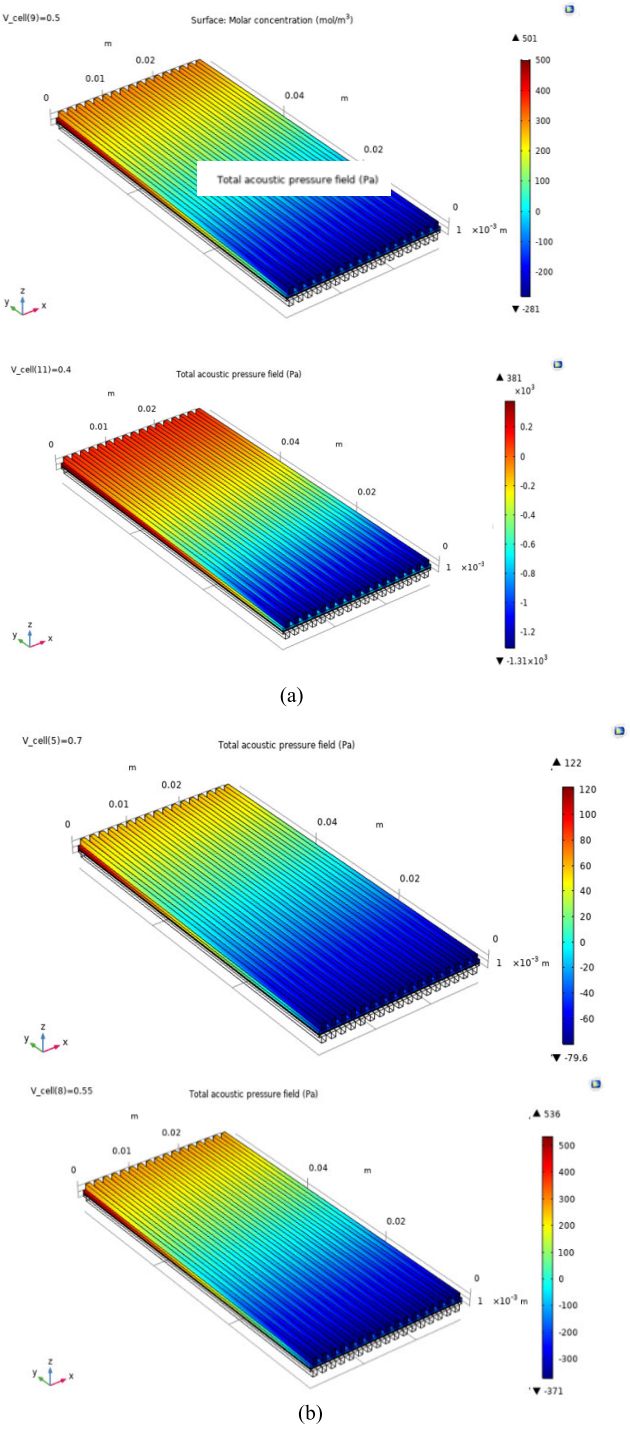


**FIGURE 5.** a. AE at 40 % and 60% load values. b. AE activity at 80 % and 100% load values.

deemed adequate since it encompassed all AE frequencies from the transducer useful for monitoring the AE signals from PEMFC and avoided interference from other laboratory environment. Although the amplifier was rated to 5 MHz, the upper frequency of the signal was limited by the response of the transducer.

The gain of the amplifier was switch selectable over the range 0–40 dB in 1 dB steps. This was connected to

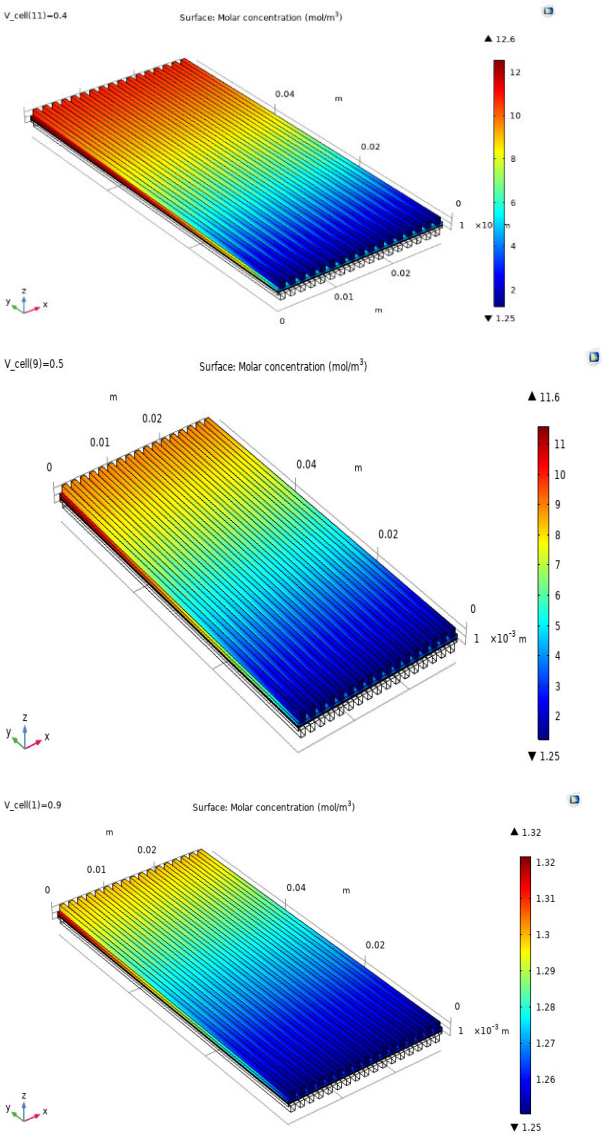


**FIGURE 6.** Water activity at the anode side under different load conditions.

the input of a GDS-1102-GW Instek Digital Oscilloscope. A sampling interval of 200 ns was used for all experiments and 1024 points were required per signal. The scope was retriggered such that approximately 100 points were collected before the **next** trigger point. The digital data resolution were transferred to a personal computer via a data acquisition card and stored on a hard disk for future processing.

The PEMFC was tested under six loads, the first test was conducted without applied load (open circuit) and then five other tests were conducted linearly increasing the load stepwise.. In order to classify AE activity, data was band pass filtered into three different frequency bands: a low frequency band (20–100 kHz), a medium frequency band (100–500 kHz), and a high frequency band (500–1000 kHz). Due to the difficulty of extracting information from the

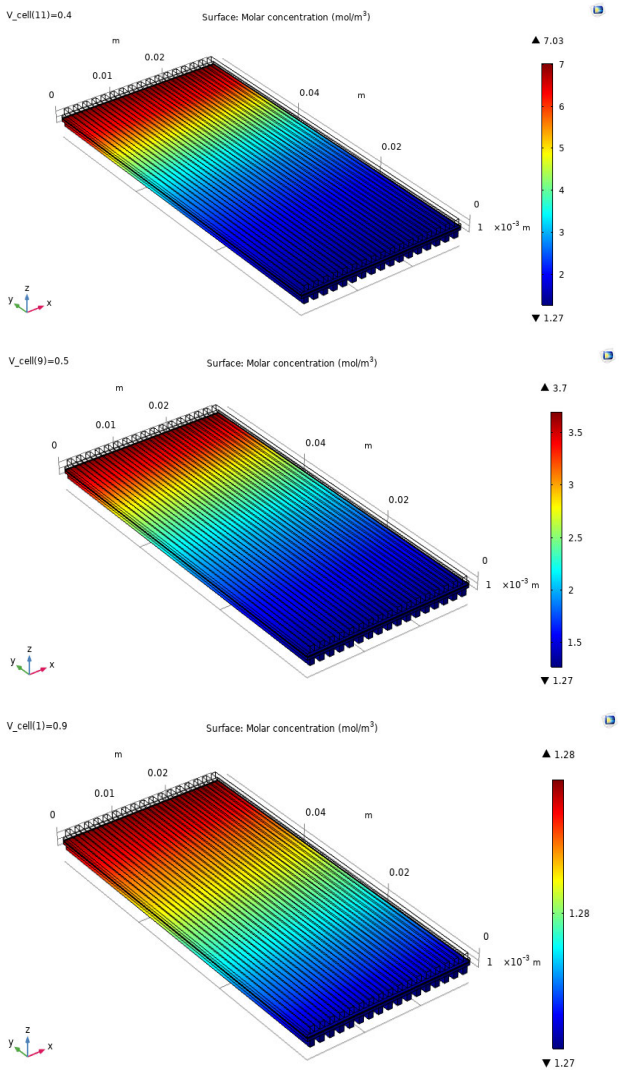


**FIGURE 7.** Water activity at the cathode side under different load conditions.

signals in the time domain, the Fast Fourier Transform (FFT) was used to transform the signal to the frequency domain [19]. This allowed the AE signal to be investigated using relatively simple statistical methods to extract information from the AE data, to be used as a condition-monitoring tool.

Calculating the root mean square (RMS), kurtosis, and skewness values of the AE signals could provide a quick way to analyse the PEMFC in a relatively straightforward way. Using such indicators, information on the PEMFC's condition could be assessed without the need for any special training of staff.

A user-defined code in the MATLAB environment was written for data analysis in both time and frequency domains. A block diagram of the AE signal acquisition and pre-processing procedure is shown in Figure 4a and the experimental components are shown in Figure 4b.

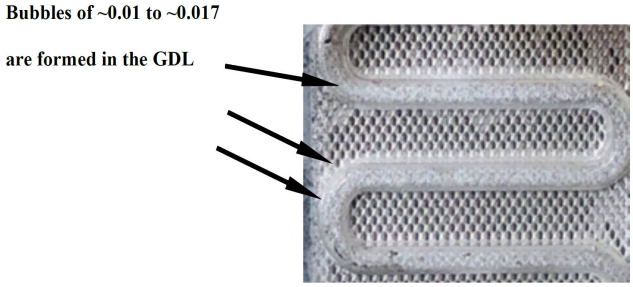


**FIGURE 8.** Photo of water bubbles in GDL and gas channels.

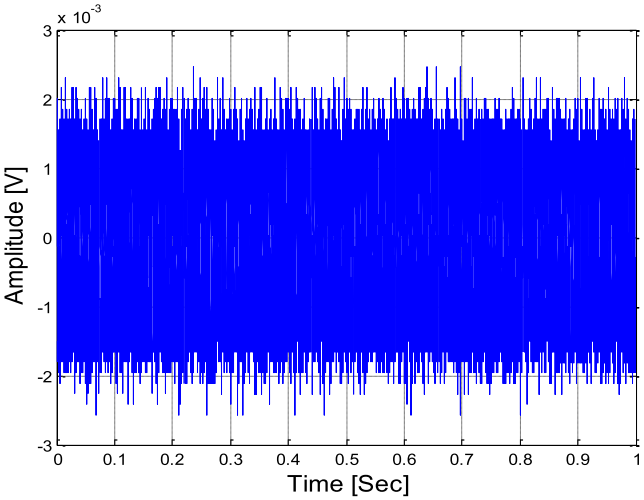


**FIGURE 9.** AE signal in the time domain with no load.

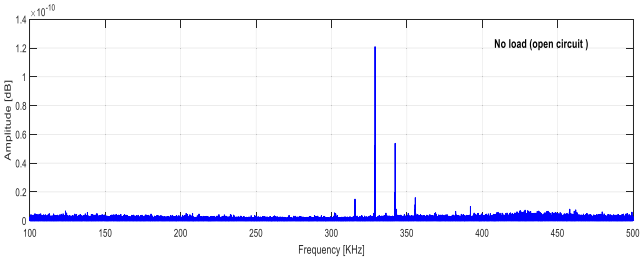


**FIGURE 10.** Acoustic emission in frequency domain.

## V. RESULTS AND DISCUSSION

Figure 5 depicts a 3-dimensional finite element model using the COMSOL software package to predict AE signals at different temperatures and pressures. The assumptions made in the model were:

a) The electrode layer was ultrathin; hence, the diffusion of the gas in the electrode layer could be neglected.
b) An ideal gas mixture was used.
c) Any liquid water formed as small droplets.
d) The electro-osmotic diffusion coefficient and coefficient of diffusion for water in the membrane were determined primarily by the water activity in the channel of the anode flow, especially in places with high current densities because in this state it was most likely that the

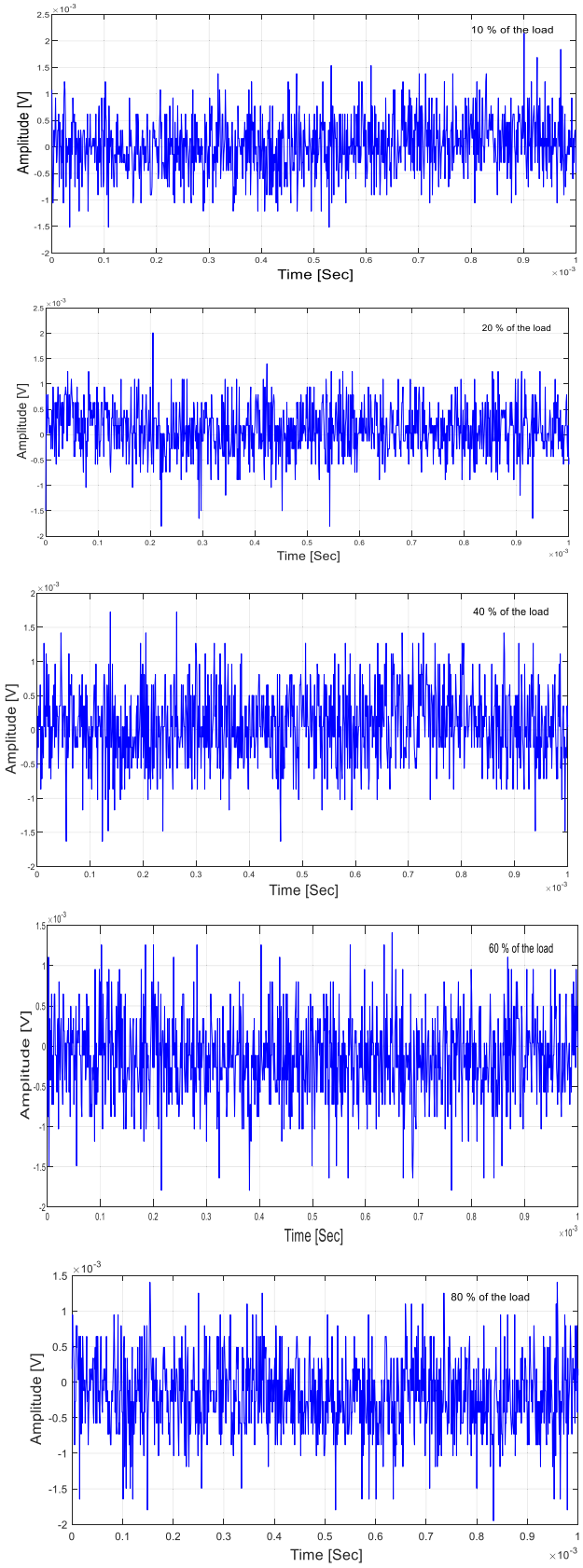


**FIGURE 11.** Acoustic emission in time domain under different loads.

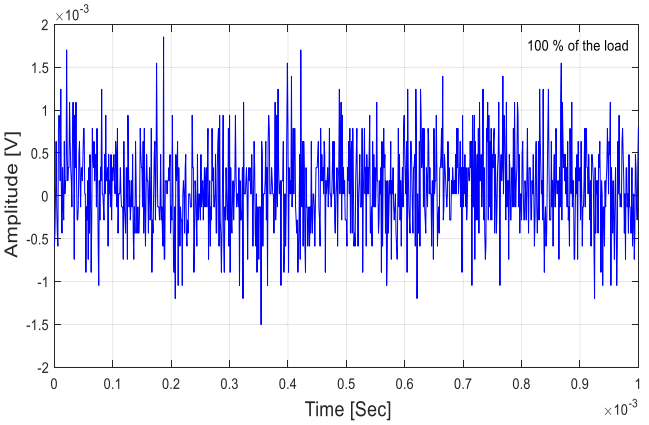


**FIGURE 11.** *(Continued.)* Acoustic emission in time domain under different loads.

anode side of the membrane was drier than the cathode side.

Several methods can be used to control the electrochemical reactions in PEMFC, for example by increasing the flow rate of the reactants. There is a close relationship between the water produced and electrochemical reaction as mentioned early. In this work, the load variation was used to investigate the AE signals generated as a result of water bubbles.

Figure 5(a and b) illustrates the AE activities at 40 %, 60 %, 80 %, and 100 % of the PEMFC's full load. The figure shows the AE signals with a change of load value.

Figure 6 and Figure 7 show the water activity at anode and cathode sides, respectively of the cell under different operating conditions.

**TABLE 2.** Data collected from the 500 mW PEMFC unit.

| Load % | Voltage (V) | Current (A) | Power (mW) |
|---|---|---|---|
| 0 | 1.1 | 0 | 0 |
| 20 | 0.32 | 1.43 | 457.6 |
| 40 | 0.76 | 0.22 | 167.2 |
| 60 | 0.84 | 0.08 | 67.2 |
| 80 | 0.94 | 0.01 | 9.4 |
| 100 | 0.97 | 0.01 | 9.7 |

Table 2 lists the measured values collected from the 500 mW PEMFC unit for various resistive loads.

Figure 8 shows the water accumulates at the cathode side in GDL and gas channels as a result of electrochemical reactions and electro-osmotic drag phenomenon. The volume of the formed bibles was observed to vary from 5.3787e-06 $mm^3$ to 1.2750e-05 $mm^3$ (radius of 0.01 mm to ∼0.017 mm). Based on the mathematical modelling, the formed bubbles and events are expected to generate a frequency range from ∼500 kHz to 800 kHz. This is demonstrated and clearly shown on the experimental results.

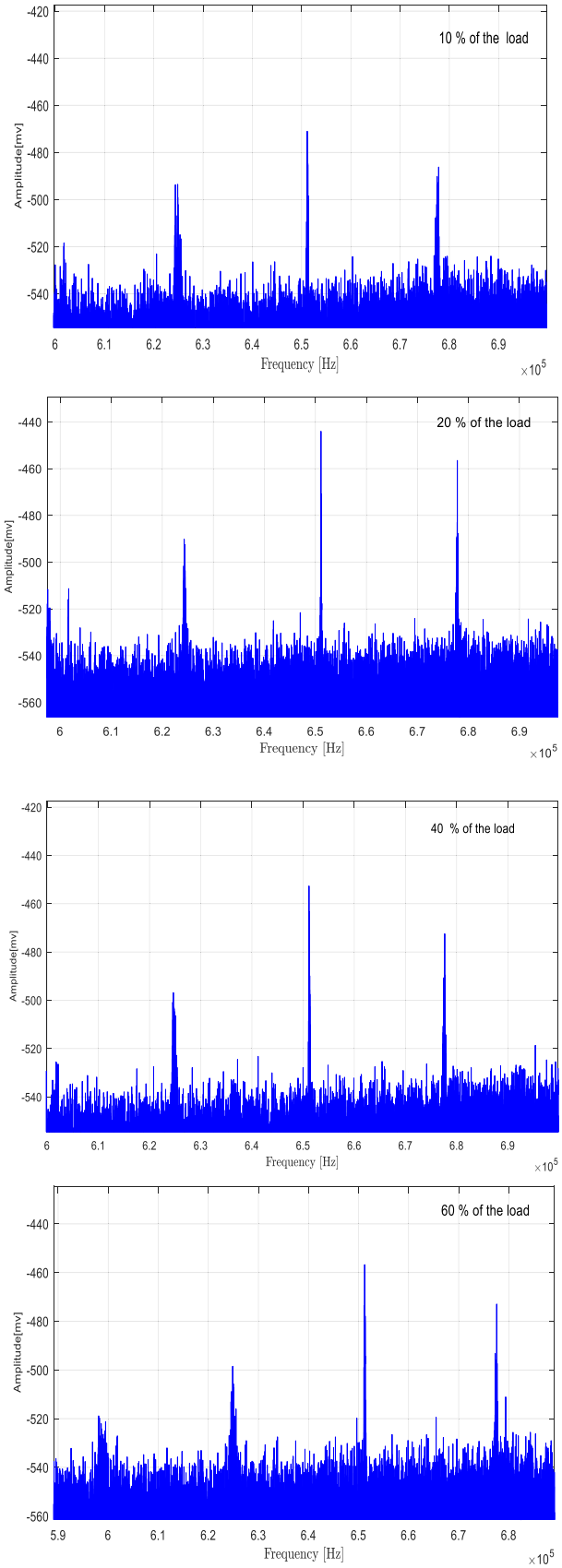


**FIGURE 12.** Acoustic emission in frequency domain under different loads.

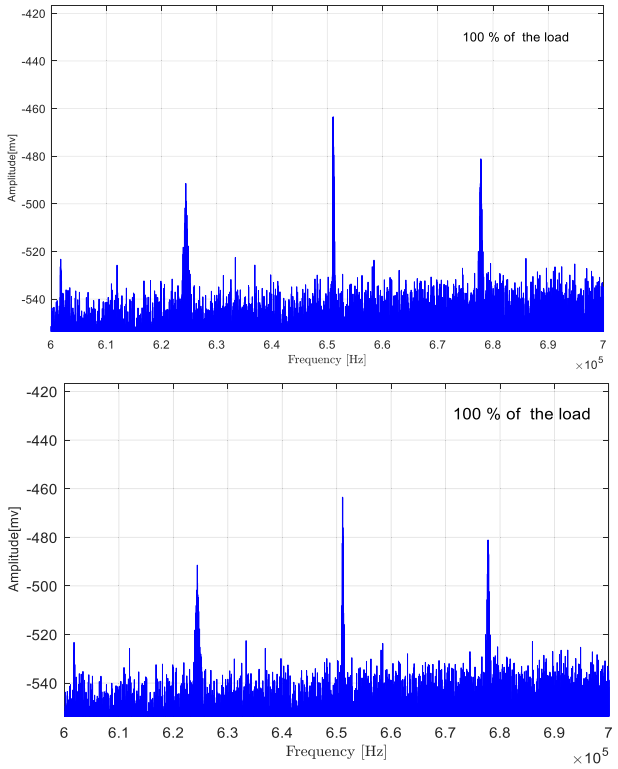


**FIGURE 12.** *(Continued.)* Acoustic emission in frequency domain under different loads.

The time domain output of an AE transducer attached to the 500 mW FC with no load (open circuit) is shown in Figure 9. The AE signals to noise ratios were enhanced by averaging and filtering out unwanted noise.

Figure 10 presents the frequency domain of the signal obtained from the cell when the cell was in open circuit condition and no current flowed. As shown in Figure 10, the main features in the AE waveform are the peaks corresponding to random signals and because of the internal resistance of the cell.

Figure 11 and Figure 12 show the time and frequency domains for each of the six different loads. It can be observed that the amplitudes of the time domain waveforms increased as the load increased.

The highest peak is observed at the resonance frequency of the AE transducer (652 kHz), while the other peaks are multiples of this main frequency component. The amplitudes of any higher harmonics can be ignored because they contain considerably less energy than the first leading term. The amplitude of the peaks increased with load increments and the frequency at which the peak occurred also rose in direct proportion to the increase in load.

Figure 13 shows the histograms for the five different loads, and the results indicate that the data is not close to a Gaussian distribution, and that standard deviation (SD) and other common statistical parameters, such as peak and RMS values,

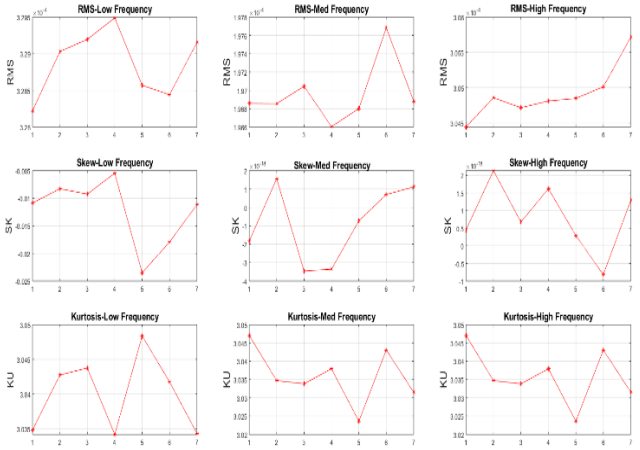


**FIGURE 13. Load variation effects on various statistical factors for different frequency bands.**

skewness, and kurtosis, are not good measures to evaluate the differences between the various histograms. It can be seen that the histograms for the AE signals have a similar distribution for different levels of current.

## VI. CONCLUSION

In this study, the effect of load operating conditions on acoustic emission signals induced in PEMFCs have been investigated. Model-based simulated results under different operating parameters were demonstrated and interpreted. In addition, data collected from a 500 mW PEMFC unit have been analyzed and signal plots presented. The liquid water produced as a result of the reaction between the fuel (at the anode) and oxidizer (at the cathode), it is possible to identify its formation by measuring the generation of AE. Acoustic emissions generated as a result of the activity of bubbles were utilized to study the operating and health situations for the proton exchange membrane fuel cells (PEMFCs). The results from the simulation and experiments showed that increasing the load value in the experiments (pressures and/or temperatures in the simulation) led to an increase in the amplitude of acoustic emissions due to abrupt increase on bubble formation. In addition, the presented work determined that there is a strong correlation between electric loading conditions and the acoustic emissions induced by proton exchange membrane fuel cells (PEMFCs) activities. In this context, acoustic emission measurements displayed interesting results in terms of good response and high sensitivity to changes in operating conditions which makes them a promising control and condition monitoring tool.

## REFERENCES

[1] T. Ahmad and D. Zhang, "A critical review of comparative global historical energy consumption and future demand: The story told so far," *Energy Rep.*, vol. 6, pp. 1973–1991, Nov. 2020.
[2] J. Lange, J. Hilgedieck, and M. Kaltschmitt, "Renewable resources of energy for electricity generation-development trends and necessities within the overall energy system," *Jordan J. Mech. Ind. Eng.*, vol. 13, no. 3, pp. 207–220, 2019.
[3] N. L. Panwar, S. C. Kaushik, and S. Kothari, "Role of renewable energy sources in environmental protection: A review," *Renew. Sustain. Energy Rev.*, vol. 15, no. 3, pp. 1513–1524, Apr. 2011.
[4] A. Albarbar and M. Alrweq, *Proton Exchange Membrane Fuel Cells: Design, Modelling and Performance Assessment Techniques*. Springer, 2017. [Online]. Available: tps://link.springer.com/book/10.1007/978-3-319-70727-3
[5] S. Kirsten, "Renewable energy sources act and trading of emission certificates: A national and a supranational tool direct energy turnover to renewable electricity-supply in Germany," *Energy Policy*, vol. 64, pp. 302–312, Jan. 2014.
[6] C. Batunlu and A. Albarbar, "A technique for mitigating thermal stress and extending life cycle of power electronic converters used for wind turbines," *Electronics*, vol. 4, no. 4, pp. 947–968, Nov. 2015.
[7] A. Albarbar and M. Alrweq, "Effective technique for improving electrical performance and reliability of fuel cells," *Int. J. Power Electron. Drive Syst. (IJPEDS)*, vol. 8, no. 4, p. 1868, Dec. 2017.
[8] X. Zhang, T. Zhang, H. Chen, and Y. Cao, "A review of online electrochemical diagnostic methods of on-board proton exchange membrane fuel cells," *Appl. Energy*, vol. 286, Mar. 2021, Art. no. 116481.
[9] Q. Chen, G. Zhang, X. Zhang, C. Sun, K. Jiao, and Y. Wang, "Thermal management of polymer electrolyte membrane fuel cells: A review of cooling methods, material properties, and durability," *Appl. Energy*, vol. 286, Mar. 2021, Art. no. 116496.
[10] F. D. Bianchi, C. Ocampo-Martinez, C. Kunusch, and R. S. Sanchez-Pena, "Fault-tolerant unfalsified control for PEM fuel cell systems," *IEEE Trans. Energy Convers.*, vol. 30, no. 1, pp. 307–315, Mar. 2015.
[11] A. Albarbar, F. Gu, A. D. Ball, and A. Starr, "Acoustic monitoring of engine fuel injection based on adaptive filtering techniques," *Appl. Acoust.*, vol. 71, no. 12, pp. 1132–1141, Dec. 2010.
[12] A. Albarbar, F. Gu, and A. D. Ball, "Diesel engine fuel injection monitoring using acoustic measurements and independent component analysis," *Measurement*, vol. 43, no. 10, pp. 1376–1386, Dec. 2010.
[13] S. Hashimoto, H. Watanabe, T. Sakamoto, T. Kawada, K. Yashiro, J. Mizusaki, K. Kumada, D. Changsheng, K. Sato, and T. Hashida, "The design and development of an evaluation system for redox characteristics of anode supported SOFCs using *in-situ* acoustic emission and electrochemical technique," in *Proc. ASME 10th Int. Conf. Fuel Cell Sci., Eng. Technol.*, Jul. 2012, pp. 521–525.
[14] T. G. Crowther, A. P. Wade, P. D. Wentzell, and R. Gopal, "Characterization of acoustic emission from an electrolysis cell," *Analytica Chim. Acta*, vol. 254, nos. 1–2, pp. 223–234, Nov. 1991.
[15] B. Legros, P. X. Thivel, F. Druart, Y. Bultel, and R. Nogueira, "Diagnosis and modelling of proton-exchange-membrane fuel cell via electrochemical-impedance-spectroscopy and acoustic-emission measurements," in *Proc. 8th Int. Symp. Adv. Electromech. Motion Syst. Electr. Drives Joint Symp.*, Jul. 2009, pp. 1–6.
[16] L. Maier *et al.*, "Utilised the AE technique to study the gases flow inside PEMFCs[2]," in *The Study Concluded That There are Good Correlations Between the Flow Rates, Current Quantity and the Corresponding AE Parameters Measured*.
[17] S. S. Khan, H. Shareef, C. Bouhaddioui, and R. Errouissi, "Membrane-hydration-state detection in proton exchange membrane fuel cells using improved ambient-condition-based dynamic model," *Int. J. Energy Res.*, vol. 44, no. 2, pp. 869–889, Feb. 2020.
[18] D.-H. Shin, S.-R. Yoo, and Y.-H. Lee, "Real time water contents measurement based on step response for PEM fuel cell," *Int. J. Precis. Eng. Manuf.-Green Technol.*, vol. 6, no. 5, pp. 883–892, Oct. 2019.
[19] H. Ahmed, M. Benbouzid, M. Ahsan, A. Albarbar, and M. Shahjalal, "Frequency adaptive parameter estimation of unbalanced and distorted power grid," *IEEE Access*, vol. 8, pp. 8512–8519, 2020, doi: 10.1109/ACCESS.2020.2964058.
[20] M. Alrewq and A. Albarbar, "Investigation into the characteristics of proton exchange membrane fuel cell-based power system," *IET Sci., Meas. Technol.*, vol. 10, no. 3, pp. 200–206, May 2016.
[21] E. Misran, N. S. M. Hassan, W. R. W. Daud, E. H. Majlan, and M. I. Rosli, "Water transport characteristics of a PEM fuel cell at various operating pressures and temperatures," *Int. J. Hydrogen Energy*, vol. 38, no. 22, pp. 9401–9408, Jul. 2013.
[22] J. Pierre, B. Dollet, and V. Leroy, "Resonant acoustic propagation and negative density in liquid foams," *Phys. Rev. Lett.*, vol. 112, no. 14, p. 112, Apr. 2014.

**MOHMAD AL-RWEG** received the B.Sc. degree in electrical engineering from Sebha University, Libya, in 1999, the M.Sc. degree in electrical and power electronics from Bradford University, and the Ph.D. degree in renewable energy from Manchester Metropolitan University, in 2017. He has worked for more than 15 years as a research in the industry and academia. His research interests include power electronics, electrical power, fuel cells, and photo-voltaic.

**KHALED AHMEDA** received the B.Eng. degree of electrical and electronics engineering from the College of Petroleum Engineering, Al-Brega, Sirte University, Libya, in 2003, the M.Sc. degree in microelectronics from Universiti Kebangsaan Malaysia, Bangi, Malaysia, in 2005, and the Ph.D. degree in GaN HEMTs for power and RF applications. In 2006, he became an Assistant Lecturer with Sirte University. He worked as a Research Assistance with Swansea University, from 2017 to 2018, and a Research Visitor with the Nanoelectronic Devices Computational Group and the GaN Devices Modeling Group, Swansea University, from 2018 to 2020. He is currently working as an Associate Tutor with the Cardiff School of Technologies, Cardiff Metropolitan University. His current research interests include modeling of III-nitrides-based devices, SiC MOSFET, reliability, and characterization of GaN HEMTs.

**ALHUSSEIN ALBARBAR** (Member, IEEE) has worked for more than 27 years as a research and development leader with both power industry and academia. He is currently a Professor of sustainable systems engineering with the Department of Engineering, Manchester Metropolitan University, U.K. Until, he has supervised over 25 research degrees, including 17 doctoral studies. He led and participated in well over 7M worth of projects. Deliverables of those projects are cost-effective solutions to reduce the carbon print of industrial, commercial, transportation, and public buildings to mitigate global warming related issues. He has published more than 100 articles and papers in refereed journals and international conference proceedings, three books and five-book chapters. His current research interests include novel control and diagnostic strategies for Industry 4.0 applications, sustainable and renewable power systems, smart sensing, intelligent control, and monitoring algorithms used for electromechanical power plants.